Xenocrystic richterite in an olivine–nephelinite: destabilisation and diffusion phenomena

CHRISTIANE WAGNER,[1] ABDELKADER MOKHTARI[1,2] AND DANIELLE VELDE[1]

[1] Laboratoire de Pétrologie Minéralogique, (URA 736 du CNRS) U.P.M.C.–Paris 6, 4 Place Jussieu, Tour 26, E3, 75252 Paris Cedex 05, France
[2] Laboratoire de Géologie, Université de Meknès, Morocco

Abstract

A partly destabilised Na-richterite has been found in an olivine–nephelinite from Morocco. The richterite crystal (600 × 420 μm) is surrounded by a reaction zone (400–700 μm) of K- and Si-rich glass containing small (<50 μm) olivine ($Fo_{80-83\%}$) and endiopside crystals. Outwards, another zone is formed of normal magmatic minerals and circumscribes the original crystal, indicating that the destabilisation event took place at the end of the crystallisation sequence. Estimated ascent time of about 100 hours would have completely decomposed an isolated richterite crystal, which suggests that the amphibole was originally included in a xenolith. A mass-balance calculation shows that the richterite isovolumic decomposition was accompanied by exchanges with the magma. The loss of Na from the reaction zone and the gain of Al from the magma allowed the precipitation of an analcime-rich zone observed around the destabilised amphibole and the concentration of K in the reaction zone glass. Compositional variations, Fe and Ti increase and Mg, Ca and F decrease at the richterite edge are interpreted as the result of a diffusion process. No alkali gradients are observed. The diffusion phenomenon lasted less than 100 hours and ceased to be operative at a temperature of 900–950 °C, i.e. just below the solidus temperature. Diffusion coefficients for the amphibole are proposed: e.g 10^{-9} cm^2 s^{-1} for K_2O and 10^{-10} for FeO at 900 °C.

KEYWORDS: richterite, olivine–nephelinite, destabilisation, diffusion, Morocco.

Introduction

THE low pressure resorption of phenocrystic or xenocrystic amphiboles (mostly hornblende and kaersutite) in basaltic magmas is well-documented (since Lacroix, 1893): it results in either coronitic pseudomorphs comprising clinopyroxene, plagioclase and magnetite, or a complete replacement of the crystals. This study deals with the destabilisation of a xenocrystic richterite, a sodic–calcic amphibole, which exhibits a marginal breakdown zone of glass including small olivine and clinopyroxene crystals. Moreover, the relic part of the crystal shows compositional variations at the edge.

The richterite was found in an olivine–nephelinite from the Taourirt area (Northern Morocco), where numerous Eocene sills and dykes of basic alkaline rocks intrude the sedimentary basement (Charlot *et al.*, 1964). The olivine–nephelinite dyke outcrops on the other side of the river Za from the Ferme Dubois locality (Fig. 1 of Mokhtari and Velde, 1988), at x = 725.60 and y = 430.25 on the Taourirt sheet of the 1:50 000 Moroccan map. The rock studied has a porphyritic texture and comprises olivine and clinopyroxene phenocrysts (1 × 0.6 and 1.5 × 1 mm respectively) in a groundmass of small (<100 μm) clinopyroxene, mica, nepheline, analcime, Ti-magnetite and rare apatite crystals but lacking any amphibole crystallised with these minerals. Besides richterite, the rock also contains numerous xenocrysts: olivine, clinopyroxenes, mica and spinels. Similar xenocrystic assemblages, without richterite, are common in associated lamprophyres from this area and have been described by Mokhtari and Velde (1988).

The purpose of the present paper is to describe the reaction of the xenocrystic amphibole in a low-pressure and high-temperature environment. After a summary of the mineralogy of the lava, we will examine first the composition of the richterite followed by the study of its partial decomposition products and an estimate of the exchanges with the nephelinite magma during the reaction. Physical conditions (P,T) and duration of the

Mineralogical Magazine, September 1993, Vol. 57, pp. 515–525

richterite destabilisation will be discussed. The compositional gradients observed in the richterite will then be analysed and an attempt at estimating diffusion coefficients will be made.

Analytical methods

Electron microprobe analyses were performed with an automated Camebax. Acceleration voltage was 15 kV and current intensities 40 nA for olivine and clinopyroxene, 10 nA for amphibole and mica, 5 nA for nepheline, analcime and glass; for oxides the experimental conditions were 20 kV and 40 nA. Counting times were never less than 20 s. Standards were metal oxides or natural minerals.

Mineralogy of the lava

Clinopyroxene (54% in volume) is Al- (0.27–0.51 atom p.f.u.) and Ti- (0.07–0.17) rich Cr-free diopside (Fig. 1). The unaltered forsteritic (Fo_{88}) *olivine* (10%) is Ni-rich (0.2–0.3 wt.% NiO). The rare (2%) hydroxylated phase is *phlogopite* with mg* = 70–77, mg* expressed as 100 Mg/(Mg + Fe); it has low Si (5.2–5.4 a.p.f.u.) and high Al (2.4–2.8 a.p.f.u.) contents and is rich in TiO_2 (up to 7.0 wt.%) and BaO (3–10.5 wt.%). *Nepheline* (15%) forms large (up to 400 μm) crystals and *analcime* (5%) poikilitic patches including late-crystallising clinopyroxene and Ti-magnetite. The composition of nepheline varies from $Ne_{59}Ks_{13}Qz_{28}$ to $Ne_{74}Ks_{20}Qz_6$ in mole%. Analcime shows little variation from the theoretical formula. *Titanomagnetite* (14%) contains high TiO_2 (21–24 wt.%) and low Al_2O_3 (2–3 wt.%), MgO (2–4 wt.%) and Cr_2O_3 (<100 ppm) contents. Representative analyses are listed in Table 1.

Destabilisation of the xenocrystic richterite

Richterite, $NaCaNaMg_5Si_8O_{22}(OH,F,Cl)_2$ is a sodic–calcic amphibole with a composition controlled by the liquid composition (Charles, 1977). The host rocks for richterite show peculiar characteristics, such as Al-deficiency and normative metasilicate ± quartz, far from that of the nephelinite (Table 2). Richterite cannot have crystallised from the Al-oversaturated nephelinite magma (Na + K)/Al = 0.57) and is considered to be of xenocrystic origin. It should be noted that richterite has not been reported as an inherited amphibole in igneous rocks.

A single richterite crystal (600 × 420 μm) has been found. It is surrounded by a 400–700 μm wide zone, in which euhedral small (<50 μm) clinopyroxene and olivine crystals coexist with glass (Fig. 2). The crystals appear to be oriented along the direction of the amphibole cleavage. At the edge of the zone numerous small (5 μm) olivine and clinopyroxene crystals are observed. Around this zone minerals crystallised in place (clinopyroxene, olivine, nepheline, analcime, mica and magnetite) with compositions identical to those found in the nephelinite have crystallised. Analcime is more abundant in the immediate vicinity of the amphibole reaction zone (Fig. 2*a*).

The destabilisation only occurs at the crystal boundary and not within the amphibole. It is interpreted as the result of incomplete reaction with the nephelinite magma.

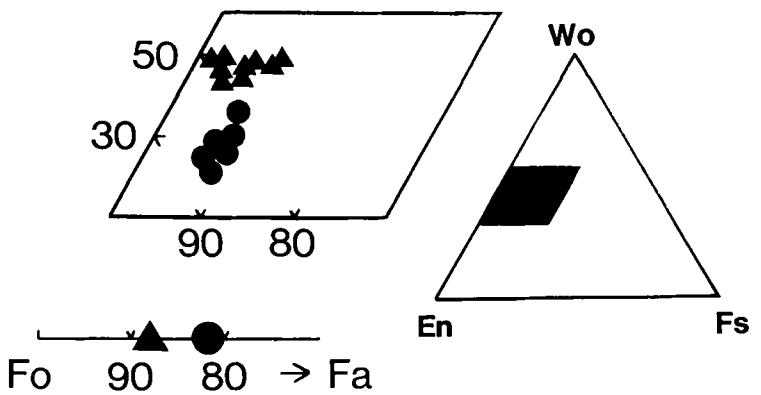

FIG. 1. Position of clinopyroxenes in a Wo–En–Fs diagram (atomic per cent) and Fo content (%) of coexisting olivines. Solid triangles: normal magmatic pyroxenes and olivines, solid circles: pyroxenes and olivines from the reaction zone around the xenocrystic richterite.

Table 1. Representative analyses of pyroxenes (1, 2), olivine (3), nepheline (4), analcime (5); xenocrystic richterite core (6) and edge (7); breakdown products after richterite: olivine (8), pyroxene (9), glass (10, 11).

	1	2	3	4	5	6	7	8	9	10	11
SiO_2	45.21	40.10	40.51	43.84	54.26	55.70	54.24	39.35	54.48	62.63	58.05
TiO_2	3.57	5.81				1.25	2.32		0.22	0.36	0.25
Al_2O_3	7.42	11.43		33.86	23.82	0.49	0.95		0.09	12.91	10.85
FeO	6.62	7.46	11.68			3.85	5.95	16.08	5.02	5.34	8.33
MgO	12.23	10.21	47.17			21.25	19.30	43.46	18.59	2.28	7.51
MnO	0.10	0.03	0.14			0.16	0.19	0.41	0.26	0.10	0.11
NiO			0.32					0.07			
CaO	23.91	23.44	0.22	1.81	0.11	6.56	6.18	0.22	19.33	0.09	0.14
Na_2O	0.38	0.39		13.29	11.96	5.50	5.48		0.49	0.16	0.40
K_2O				5.45	0.35	2.26	2.17			14.12	11.51
Cr_2O_3			0.03						0.58		
F						2.22	1.50			0.11	
FeO	2.98	3.13							4.86		
Fe_2O_3	4.05	4.81		1.06					0.17		
Total	99.85	99.35	100.07	99.31	92.50	98.30*	97.65*	99.59	99.07	98.10*	97.15
Si	1.693	1.524	1.001	8.398	2.055	7.860	7.755	0.999	1.999		
Ti	0.101	0.166				0.133	0.249		0.006		
Al	0.327	0.512		7.646	1.025	0.082	0.160		0.004		
Fe^{2+}	0.093	0.099	0.242			0.454	0.711	0.341	0.149		
Fe^{3+}	0.114	0.138		0.153					0.005		
Mg	0.682	0.578	1.739			4.469	4.112	1.644	1.016		
Mn	0.003	0.001	0.003			0.019	0.023	0.009	0.008		
Ni			0.006					0.001			
Ca	0.959	0.954	0.006	0.372	0.004	0.992	0.947	0.006	0.760		
Na	0.028	0.029		4.937	0.847	1.505	1.519		0.035		
K				1.332	0.015	0.407	0.396				
Cr			0.001						0.017		
F						0.991	0.678				
mg*	77	71	88			91	85	83	87	43	61

(*) Total minus F, Cl=O. Formulae calculated on 4 O atoms for olivine, 6 for pyroxene, 23 for amphibole, 32 for nepheline, 7 for analcime. mg* = 100Mg / (Mg+Fe total).

Table 2. Chemical composition and CIPW norm of the nephelinite.

SiO_2	40.84	Or	1.47
Al_2O_3	12.85	An	15.00
Fe_2O_3	4.23	Lc	4.27
FeO	6.53	Ne	16.96
MgO	12.36	Di	33.70
CaO	12.40	Fo	11.62
Na_2O	3.70	Fa	1.47
K_2O	1.17	Ma	6.13
MnO	0.17	Ilm	6.08
TiO_2	3.20	Ap	1.35
P_2O_5	0.57		
L.O.I.	1.96		
Total	99.98		

Richterite composition

The nephelinite xenocrystic amphibole is a potassian richterite with substantial F (0.99 a.p.f.u.) just too low to be fluor prefixed ($\geq$1.00 F) and with a high mg* of 91 (Table 1). The amount of Fe^{3+} appears insignificant. As is commonly observed in richterite from lamproites and some upper mantle nodules in kimberlites (Dawson, 1987), the tetrahedral site is incompletely filled with Si and Al (Si + Al = 7.8–7.9 a.p.f.u.) when structural formulae are calculated on the basis of 23 oxygens. TiO_2 content is about 1.25–1.50 wt.% in the core of the crystal but reaches 2.32 wt.% in the outer part which is also richer in iron (mg* = 85), suggesting the $3\,Mg = \Delta + Ti + (Fe^{2+}, Mn)$ substitution (Fig. 3*a*). As the theoretical charge in the C-group of an amphibole is equal to 10 and

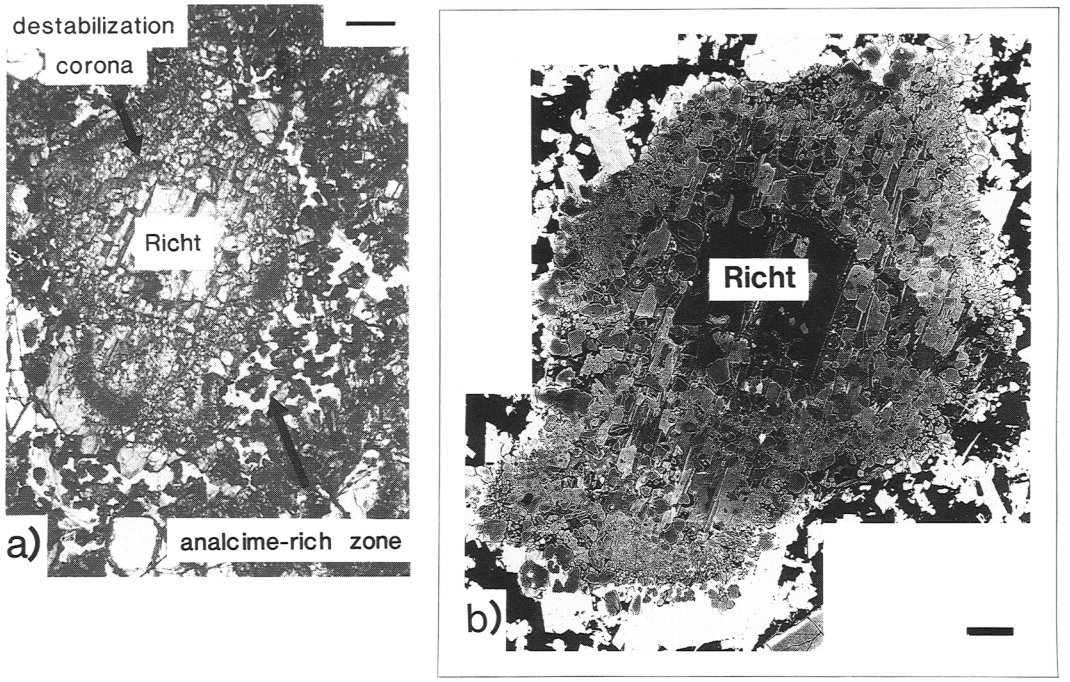

FIG. 2. Xenocrystic richterite and its reaction rim. (*a*) The destabilisation zone around the richterite crystal is surrounded by an analcime-rich zone (white). Plane polarised light. Scale bar: 200 μm. (*b*) Back-scattered electron image. Coronitic zone: olivine, dark grey rounded crystals and clinopyroxene, medium grey elongated crystals embedded in dark glassy patches. Scale bar: 90 μm. Richterite: (Richt).

considering that Mg, Fe, Mn and Ti are the C-group cations, the charge balance relation Mg(2+) + Fe(2+) + Mn(2+) + Ti(4+) = 10 is satisfied. The substitution mechanism proposed above is compatible with the 2Mg *vs.* 4Ti + 2Fe + 2Mn diagram (Fig. 3*b*), where the slight discrepancy observed between the analytical data trend and the theoretical one may be due to the presence of one of the above cations in tetrahedral position. F content is higher in the core, up to 2.22 wt.% instead of 1.50 wt.% in the rim.

Destabilisation reaction

The richterite reaction zone is comprised of olivine, pyroxene and glass. A surface imaging technique on SEM photographs gives 37% olivine, 30% pyroxene and 33% glass by volume.

Composition of the destabilisation products (Table 1): *Clinopyroxene* is endiopside (Fig. 1). It is different from the remaining clinopyroxene in having low Al_2O_3 and TiO_2 (0.07–0.36 wt.% and 0.14–0.28 wt.% respectively) (Fig. 4), and high Cr_2O_3 content which varies mostly between 0.2 and 0.5 wt.% but may reach 0.7 wt.%; mg* number is high, 85–87. *Olivine*: the MgO content is lower (mg* = 80–83) and the MnO content higher (0.4 wt.%) than those of the olivines in the lava. Olivine is Ni-poor (<0.10 wt.% NiO), as could be expected for olivine resulting from the breakdown of an amphibole. *Glass*: the endiopside and olivine crystals are embedded within a greenish brown K-rich silicic glass (10–15 wt.% K_2O and 53–62 wt.% SiO_2). The glass is Mg-rich (mg* = 61, average value). The low totals of the electron microprobe analyses imply a high and variable H_2O content (3–6 wt.%). No systematic variations in composition were observed in this glass when going from the edge of the relic crystal towards the outside.

Mass-balance calculations. A comparison between the compositions of the richterite and its destabilisation products (Table 1) shows that the glass is strongly enriched in Al and K compared to the richterite, whereas Na is all but absent. The richterite cannot be the source of the aluminium and, on the other hand, Na is not found in any of the reaction products of the destabilisation. Exchanges with the nephelinite magma must have occurred. In order to quantify the element transfers within the reaction rim, a mass-balance calculation of the amphibole destabilisation (rich-

terite + liquid = olivine + cpx + glass) was conducted. Following Gresen's approach (1967), we used the equations: a ni(A) + Xi = b ni(B) + c ni(C) + ... where a, b, c are stoichiometric coefficients; ni(A) is the molar composition in element (i) of the phase A; and Xi represents the gain or loss of element (i) of the system (reaction rim) (Cotonian *et al.*, 1988). Their resolution requires two kinds of hypotheses dealing with element mobility (Xi) and volume variation during the reaction, expressed as the volume factor Fv = (b V(B) + c V(C) + ...)/a V(A), V(A) being the molar volume of phase A.

The whole set of solutions is visualised graphically on composition–volume diagrams (Fig. 5) and the solution which best limits element transfers is chosen (Potdevin and Marquer, 1987). On such diagrams, elements which are immobile have a 0 value on the y axis. We can see on the relative mobility diagram (Fig. 5*a*) that the decomposition of the richterite has necessitated exchanges with the magmatic liquid: for example

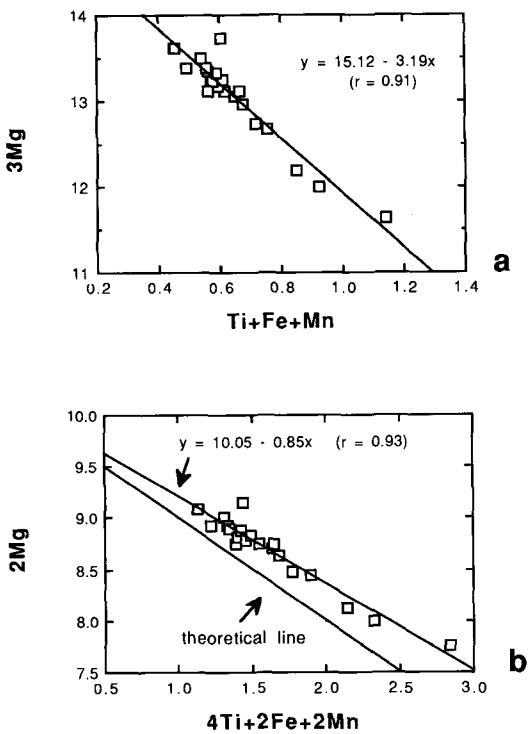

FIG. 3. The possible substitution 3 Mg = Δ + Ti + (Fe + Mn) in the xenocrystic richterite is suggested by the diagrams showing the C-group cationic occupancy (Fig. 3*a*) and the charge balance (Fig. 3*b*). On this figure the theoretical line 2 Mg + 4 Ti + 2 Fe + 2 Mn = 10 is drawn.

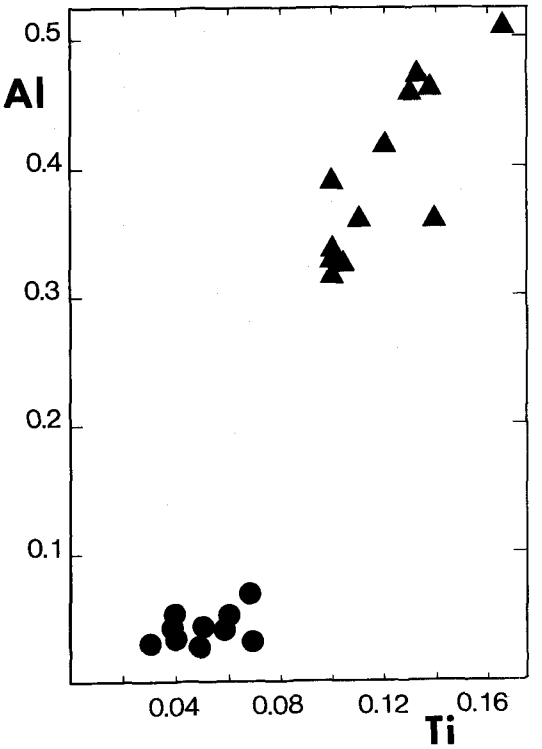

FIG. 4. Bivariate distribution of Al and Ti in clinopyroxenes. Solid triangles: normal magmatic crystals; solid circles: clinopyroxenes from the reaction zone around the xenocrystic richterite.

Na and Ti are lost from the reaction zone; Al and Fe are gained from the nephelinite magma except for very low values of Fv; Ca and O appear immobile for Fv = 1. Considering the absolute losses or gains of element (i) *vs* volume factor (Fig. 5*b*), the most limited transfers occur for an isovolumic reaction (Fv = 1), where the global exchange with the nephelinite magma during the reaction is minimal (Σ gains–Σ losses curve on Fig. 5*c*). Assuming an isovolumic reaction is in agreement with the observed uniform thickness of the reaction rim and the apparent conservation of the original crystal outlines. The destabilisation reaction of the richterite may be written for 1 mole of initial amphibole, assuming Fv = 1:

1 *amp* + 0.5 Al + 0.7 Fe + 0.6 Mg + 0.5 K
= 2.3 *olivine* + 1.2 *cpx* + 2.2 *glass* + 0.1 Ti
+ 0.5 H + 1.4 Na + 0.8 Si + 0.1 O.

Considering that the ratio (K + Na + Ca/2)/(Al + Fe^{3+}) is an approximate representation of a silicate melt structure, we can compare the 'structural state' of the nephelinite magma with

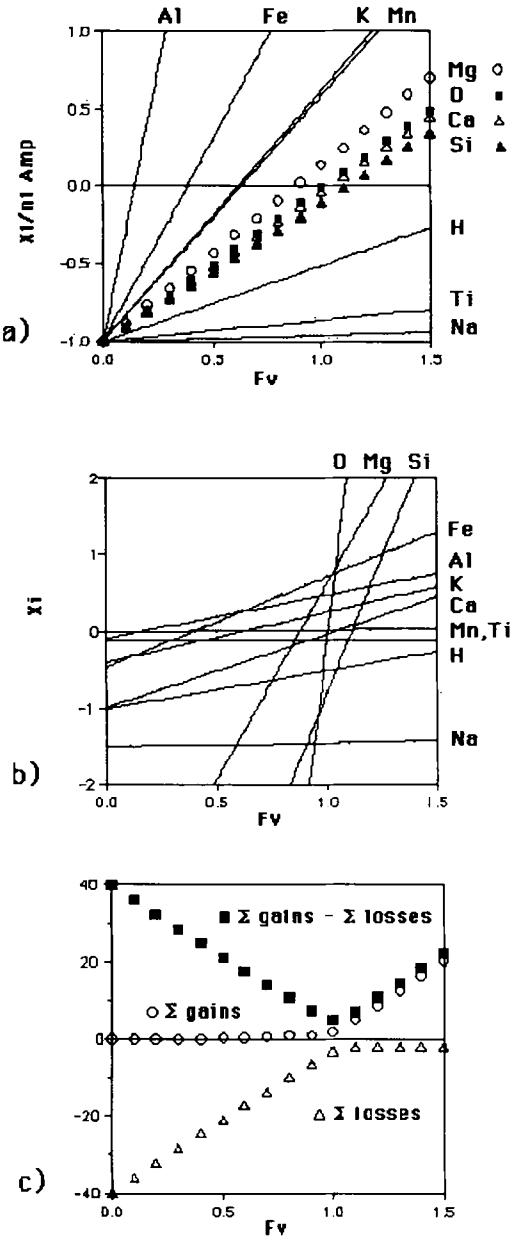

FIG. 5. Composition-volume diagrams. (*a*) Relative mobility diagram showing the gain (Xi > 0) or loss (Xi < 0) of element (i) with respect to its initial content in amphibole (ni) *vs.* the volumic factor Fv of the reaction, defined as the ratio of Volume of products/Volume of reactants. (*b*) Absolute gain or loss of element (i) at different Fv for one mole of amphibole. (*c*) Variation of the sum of the absolute gains and losses within the reaction site suggesting an isovolumic destabilisation of the amphibole.

that of the glass found in the reaction zone. They both have a similar value of 1.2, indicating a structural equilibrium. On the other hand, the liquid which would have resulted from the richterite melting shows a very high value between 12 and 23.5 (values calculated from the amphibole rim and centre composition respectively, assuming that all Ca is incorporated in the clinopyroxenes and all iron is ferrous). To diminish this ratio from a value >12 to 1.2 can be done by increasing Al or decreasing alkalis, which corresponds to Al transfer from the magma to the reaction zone and alkali loss. This allows for the precipitation of an Al and alkali-rich phase at the interface between the reaction zone and the nephelinite magma. An analcime-rich zone is indeed present around the destabilised amphibole (Fig. 2*a*). The crystallisation of analcime increases the K/Na ratio of the residual liquid, explaining the high K-content observed in the glass.

P, T and t constraints bearing upon the destabilisation of richterite

Experimental breakdown results. The thermal stability of the richterite depends on its Fe–Mg composition. For the richterite under discussion ($Mg_{4.5}Fe_{0.5}$), maximal thermal stability of OH–Na-richterite lies between 1025 ± 5 °C (for Mg_5) and 985 ± 10 °C (for Mg_4Fe) at 1 kbar, for oxygen fugacities determined by the QFM or H–Mt buffer (Charles, 1977). The introduction of F should raise the thermal stability of richterite but data are available only for F–K–Mg_5 richterite, which is stable up to 1160 °C at 1 atm. (Gilbert and Briggs, 1974). A 1000–1100 °C temperature is considered as representing the upper stability limit for a $Mg_{4.5}Fe_{0.5}$ amphibole which contains some F. However, as the xenocrystic richterite reacts with the nephelinite magma, the destabilisation temperature must have been lower.

At pressure above 150 bars and up to 1 kbar the Mg_5 richterite melts incongruently to a diopside–forsterite–enstatite melt assemblage, whereas the decomposition of Mg_4Fe richterite produces magnetite in place of enstatite (Forbes, 1971; Charles, 1975 and 1977). In the experimental breakdown of the Mg_4Fe richterite on QFM buffer, the olivine composition has been estimated at Fo_{84}, the glass appears to contain only Na and Si, but the clinopyroxene composition has not been determined (Charles, 1977). The Fo content of the olivine found in the reaction zone is similar, whereas the glass is K-rich but Na-free and thus does not reflect the Na/K ratio of the richterite. Neither enstatite nor oxides were observed among the destabilisation products: the

Moroccan richterite did not contain enough iron to allow the crystallisation of magnetite whereas enstatite is unstable in a silica-undersaturated nephelinite magma.

Considering experimental results obtained by Tilley and Thompson (1972) at atmospheric pressure for a Hawaiian nephelinite whose bulk composition is close to that of the present specimen, it appears reasonable to suppose for the nephelinite a liquidus temperature of 1305 °C and a solidus at 1085 °C. The temperature of the magma may then be considered high enough to destabilise the xenocrystic richterite.

Duration of the amphibole destabilisation event. Experiments of isothermal constant-rate decompression breakdown of hornblende in dacitic lavas were performed at 900 °C, from 160 to 2 MPa by Rutherford (1990; see also Rutherford and Hill, 1993). The breakdown rim is made of pyroxene, Fe–Ti oxide, plagioclase and glass. After a slow initial development of the reaction rim, the rate of dissolution of the amphibole is constant around $3–6 \times 10^{-9}$ cm s^{-1}. Using these results, the dissolution of a 400 μm wide zone of richterite may have lasted 80–150 days. However, this low rate seems inadequate for two reasons: firstly, the dissolution rates vary exponentially with ΔT (Donaldson, 1985). The experiments were conducted at 900 °C while the temperature of the nephelinite magma was higher. Secondly, the dissolution rate is related to the instability of a given mineral in the melt; the richterite is highly unstable and is likely to dissolve rapidly in the nephelinite Al-saturated magma.

On the other hand, assuming that the richterite dissolution rate (V) was controlled by the interdiffusion of Al and alkalis between the reaction zone and the nephelinite magma, we can estimate V if we know the time (t) required to destabilise a given width (x) of richterite. The time can be estimated from the diffusion equation $x = 2\sqrt{Dt}$, where x is an estimate of the distance of the diffusion front and D the diffusion coefficient (Shaw, 1974). As Na is a very mobile element, Al diffusion will be the limiting factor. For a distance of 400 μm and $D(\mathrm{Al}) = 10^{-8}$ to 10^{-9} cm^2 s^{-1} at 1200 °C and 1100 °C (Jambon, 1983), t varies between 10 and 100 hours. Reporting these values in the first equation leads to a dissolution rate of 10^{-6} to 10^{-7} cm s^{-1}. The time required to allow the complete dissolution of the richterite crystal (1.1 × 1 mm) would then have been between 25 and 250 hours.

We can propose limits for the duration of the ascent of the nephelinite magma. The minimum velocity of ascent of a basaltic liquid carrying peridotite inclusions is 1–2 km h^{-1} (Kushiro *et al.*, 1976), i.e. the rise of the basaltic magma from a depth of 50 km to the surface lasts less than 60 hours. A magma of a nephelinite composition has a lower viscosity; however, the conservation of the reaction zone and of the analcime-rich zone suggests that the nephelinite magma was highly viscous, i.e. contains at least 50% crystals, at the time of the reaction. An ascent time of about 100 hours would have almost completely decomposed the richterite crystal.

We may then conclude tentatively that the conditions allowing the amphibole to remain partly intact are its inclusion in a polycrystalline aggregate whose ultimate disruption intervened at the time of emplacement. The nature of this aggregate is likely to be an upper-mantle nodule, as indicated by the composition of the richterite (Dawson and Smith, 1982). Such nodules also contain diopside, a fast dissolving mineral (Brearley and Scarfe, 1986), which would have totally disappeared.

Diffusion phenomena in the richterite crystal

Concentration profiles

The richterite crystal shows compositional variations towards it edges. FeO, TiO_2, CaO, MgO, Na_2O, K_2O and F profiles are given in Fig. 6. The different elements with the exception of Na and K have similar profile with an inflexion situated at the same distance from the edge of the crystal. These chemical gradients are interpreted as being related to a diffusion process. No uphill diffusion has been observed. Several profiles made through the whole crystal indicate that the diffusion zone is limited to the outer part of the crystal. This zone corresponds to a band of stronger pleochroism which can be seen in transmitted light. No zonation has been observed near the indentation or the fracture visible on the photographs (Fig. 2), both of which would then be posterior to the diffusion event.

The diffusion zone appears slightly wider (50 μm) in a direction perpendicular to the c-axis. The amplitude of the FeO and MgO variations is similar in the two measured directions whereas the variations of TiO_2 and F are more important in a direction perpendicular to the c-axis. It is interesting to note that alkali oxides (Na_2O and K_2O) do not vary from centre to rim. Huebner and Papike (1970) have shown that alkali metals can be completely exchanged in the richterite A site at 850 °C and 1 kbar. They suggested that the rapidity of the phenomenon would permit the modification of the alkali ratios in natural amphibole. We may thus consider that alkali metals in

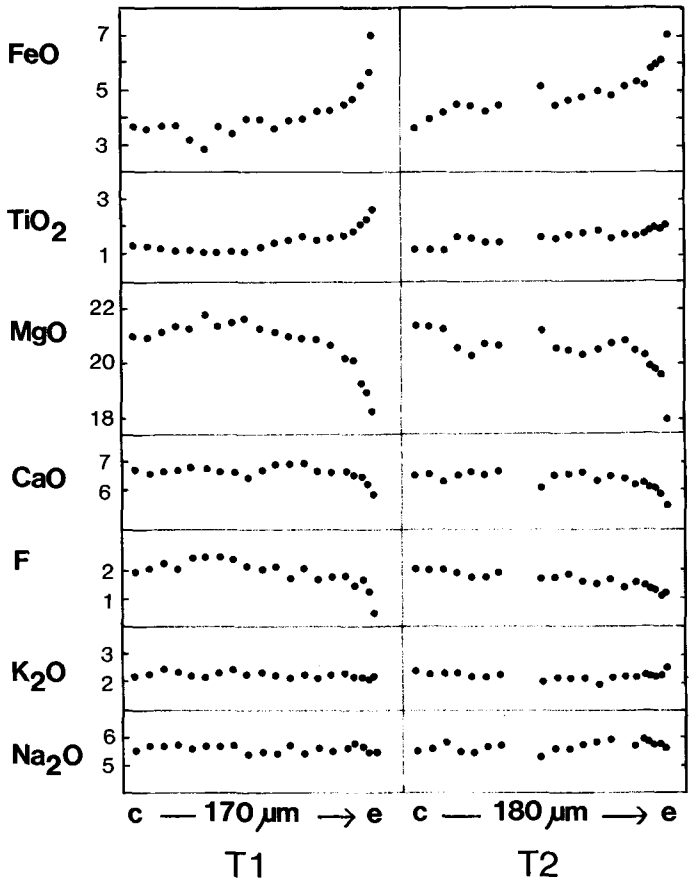

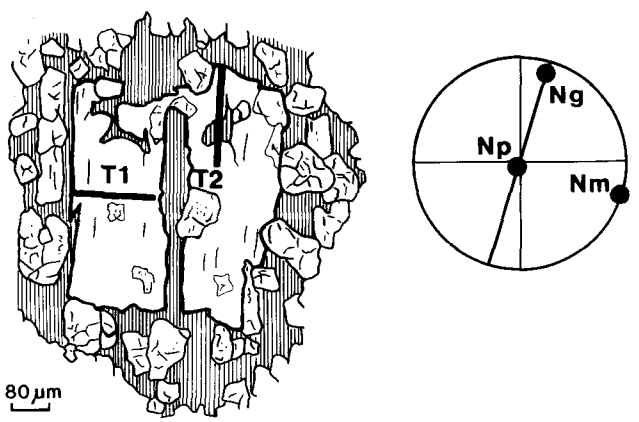

FIG. 6. Variations of oxides composition (%) in the xenocrystic richterite along two different directions T1 and T2, drawn on the crystal sketch. In both directions, the centre (c) of the crystal is on the left and the edge (e) on the right. At bottom right the circle gives the orientation of the section. Precision estimated at the 95% confidence level for each element: 2σ = 3.5% for Fe, 2.5% for Ti, 1.2% for Mg, 1.6% for Ca, 5% for F, 2.6% for K and 2% for Na.

the richterite have been modified and may have been equilibrated with the surrounding melt.

Estimation of 'diffusion coefficients'

We are aware that estimation of diffusion coefficients from a natural example has to overcome several difficulties—one is that dissolution and diffusion have occurred simultaneously, leading to a moving boundary between the richterite crystal and the liquid, a problem that we do not consider in this approach; another is that the exchange of components between the richterite and the crystallising melt involves a multicomponent diffusion process. However, we used the simplified approach of regarding the system as pseudobinary, following Cooper's (1968) concept of EBDC ('effective binary diffusion coefficient').

The calculation of the diffusion coefficient for an element D(i) depends on the time during which diffusion has been active. Whatever the value (unknown) of D(i) in richterite, we can calculate its variation with decreasing temperature using the Arrhenius equation, $D = D_o\exp(-E/RT)$. This approach requires the knowledge of the activation energy for diffusion (E), which is experimentally determined. However, since, no experimental results for cation diffusion in amphibole are available, we used for E the approximate value of 220 kJ mol^{-1} which corresponds to an average value for various silicates: olivine, pyroxene, mica and feldspar (Freer, 1981), and to the activation energy for oxygen diffusion in richterite (Farver and Giletti, 1985). Reporting this value in the Arrhenius equation we can calculate the diminution of D(i) with temperature and the diminution of the distance 'x' affected by diffusion for a given time, following the approximate relationship $x^2 = Dt$. The distance 'x' is divided by 2 for a 100 °C drop in temperature beneath the solidus temperature (1000 °C), by 6 for a 200 °C drop, by 25 for a 300 °C drop and by 120 for a 400 °C drop. No significant diffusion could have occurred at temperatures below 800 °C. On the other hand, we have to take into account the cooling effect on the diffusion process. We used the relation proposed by Dodson (1973): $E/RT_c = \ln[(-AR(T_c)^2D_o/a^2)/Es]$, where A is the geometric factor (55 for a sphere), s is the cooling rate (5.6×10^{-4}° s^{-1}), a the radius of the sphere (200 μm). The estimated 'diffusion coefficients' of FeO and MgO (Table 3), whose calculation is detailed below, enable us to obtain the value of the pre-exponential factors D_o for a given temperature. The equation gives a closure temperature in the range 900–950 °C, which would indicate that the diffusion process stopped quickly after the initial stages of cooling below the solidus temperature.

Table 3. Calculated "diffusion coefficients" (D) for FeO, MgO and K_2O at different temperatures (T°C) below the solidus. (t): duration of diffusion, in hours. (D) in cm^2 s^{-1}.

T(°C)	980	900	800	600
t	10	50	100	200
DFeO	10-9.9	10-10.6	10-10.9	10-11.2
DMgO	10-9.5	10-10.2	10-10.5	10-10.8
DK_2O	10-8.3	10-9	10-9.4	10-9.6

What can be the duration of the diffusion phenomena? First we calculate the time for a 2 m-wide dyke to cool from its liquidus temperature: we use the cooling model established for a sheet of thickness $2a$, at an initial uniform temperature T_1 and the region outside the slab at an initial temperature T_o (Carslaw and Jaeger, 1959; p. 54–5): $(T-T_o)/(T_1-T_o) = \mathrm{erf}(a/2\sqrt{\kappa t})$, T being the temperature in the centre of the dyke. Assuming that the physical properties of the enclosing rock and solidified dyke are the same, and given a thermal diffusivity (κ) of 1×10^{-6} m^2 s^{-1}, the time required to cool the dyke from 1300 °C to 1000 °C is roughly 100 hours. Another 50 hours are required to cool the dyke from its solidus temperature to 900 °C.

Finally we use the model of a sphere (radius a = 200 μm) of uniform initial composition C_1 and surface concentration maintained constant C_o: C_1 was taken at the centre of the crystal, C_o at the rim of the crystal supposed to be in equilibrium with the magma. In order to approximate the width of the diffusion zone, one point of the diffusion profile as far as possible from the edge, at 50 μm, was chosen as present concentration C. The distance between this point and the centre of the sphere (r = 150 μm) corresponds to the part of the crystal that was not modified by diffusion, given an r/a ratio of 0.75. The solutions of the differential equation of radial diffusion are obtained using the curves given by Carslaw and Jaeger (1959, p. 235). For example: for FeO: C_1 = 3.5 wt.%, C_o = 7.5 wt.%, C = 4 wt.%, leading to a Dt/a^2 value of 0.01; for MgO: C_1 = 21 wt.%, C_o = 18 wt.%, C = 20 wt.%, with Dt/a^2 = 0.03. In the case of potassium (and sodium) the diffusion is presumed to have been rapid enough to wipe out all compositional differences. We shall consider that at the centre of the sphere, the compositional differences were reduced to a very

small value, i.e. the ratio $(C-C_1)/(C_0-C_1)$ is close to 1, the Dt/a^2 value is then >0.4. 'Diffusion coefficients' for FeO, MgO and K_2O calculated for different values of time (t) are given in Table 3. For diffusion active during 50 hours, we obtain $D_{FeO} = 10^{-10.6}$, $D_{MgO} = 10^{-10.2}$ and $D_{K_2O} \geqslant 10^{-9}$, all values in $cm^2\ s^{-1}$. These values do not change significantly if we consider a diffusion event lasting 100 hours, but are slightly lower for a very short diffusion time (10 hours). 'Diffusion coefficients' for SiO_2 and TiO_2 are identical to that of MgO, whereas the profiles obtained for other elements do not allow for any estimate. We observe then a difference of at least one order of magnitude between the 'diffusion coefficients' for alkalis and those for other elements.

These 'diffusion coefficients' are within the range of diffusion coefficients reported in the literature and seem to be in agreement with what is known of diffusion in silicates in general, even though this calculation is poorly constrained.

Conclusion

The richterite originated in some deep layer of the Earth and was transported by the magma and emplaced close to the surface where the magma solidified. We may assume that the richterite crytal was not extracted from a solid rock as a single crystal but was initially included within an upper mantle polycrystalline nodule. Pressure, temperature and time were such that the crystal, once isolated, decomposed partially into an olivine, clinopyroxene and glass assemblage. The destabilisation was accompanied by exchanges with the magmatic liquid. The minerals which surround the dissolution volume define the contour of the original crystal and indicate that the melting reaction took place when all phases were coprecipitating. Diffusion, which was active during a short period (<50 hours) after the solidification of the dyke, has modified the crystal composition on a small distance for most cations but completely for Na and K.

Acknowledgements

This paper has greatly benefited from discussions with M. Fonteilles and constructive reviews by A. Jambon.

References

Brearley, M. and Scarfe, C. M. (1986) Dissolution rate of upper mantle minerals in an alkali basalt melt at high pressure: An experimental study and implications for ultramafic xenolith survival. *J. Petrol.*, **27**, 1157–82.

Carslaw, H. S. and Jaeger, J. C. (1959) *Conduction of heat in solids*. Oxford University Press, p. 510.

Charles, R. W. (1975) The phase equilibria of richterite and ferrorichterite. *Am. Mineral.*, **60**, 367–74.

—— (1977) The phase equilibria of intermediate compositions on the pseudobinary $Na_2CaMg_5Si_8O_{22}(OH)_2$–$Na_2CaFe_5Si_8O_{22}(OH)_2$. *Am. J. Sci.*, **277**, 594–625.

Charlot, R., Choubert, G., Faure-Muret, A., and Hamel, C. (1964) Age des aïounites du Maroc Nord-Oriental. *C.R. Sommaire des Séances de la Soc. Geol. France*, 401–2.

Cooper, A. R. (1968) The use and limitations of the concept of an Effective Binary Diffusion Coefficient for multicomponent diffusion. In *Mass transport in oxides* (Watchman, J. B. and Franklin, A. D., eds.), NBS Spec. Publ., **196**, 79–84.

Cotonian, C., Potdevin, J.-L., Bertrand, H., and Lombardo, N. (1988) Pseudomorphoses coronitiques d'amphibole dans le trachyte de Monac (Velay Oriental). Bilan de matière et réaction magmatique. *Bull. Minéral.*, **11**, 89–95.

Dawson, J. B. (1987) The MARID suite of xenoliths in kimberlite: relationship to veined and metasomatised peridotite xenoliths. In *Mantle xenoliths* (Nixon, P. H., ed.), 465–73.

—— and Smith, J. V. (1982) Upper-mantle amphiboles: a review. *Mineral. Mag.*, **45**, 35–46.

Dodson, M. H. (1973) Closure temperature in cooling geochronological and petrological systems. *Contrib. Mineral. Petrol.*, **40**, 259–74.

Donaldson, C. H. (1985) The rates of dissolution of olivine, plagioclase and quartz in a basalt melt. *Mineral. Mag.*, **49**, 683–93.

Farver, J. R. and Giletti, B. J. (1985) Oxygen diffusion in amphiboles. *Geochim. Cosmochim. Acta*, **49**, 1403–11.

Forbes, W. C. (1971) Synthesis and stability relations of richterite $Na_2CaMg_5Si_8O_{22}(OH)_2$. *Am. Mineral.*, **56**, 997–1004.

Freer, R. (1981) Diffusion in silicate minerals and glasses: a data digest and guide to the literature. *Contrib. Mineral. Petrol.*, **76**, 440–56.

Gilbert, M. C. and Briggs, D. F. (1974) Comparison of the stabilities of OH- and F-potassic richterite, a preliminary report (abstr.), *Eos*, **55**, 480–1.

Gresens, R. L. (1967) Composition-volume relationships of metasomatism. *Chemical. Geol.*, **2**, 47–65.

Huebner, J. S. and Papike, J. J. (1970) Synthesis and sodium–potassium exchange in the richterite series $(K,Na)NaCaMg_5Si_8O_{22}(OH)_2$. *Am. Mineral.*, **55**, 300–1.

Jambon, A. (1983) Diffusion dans les silicates fondus: un bilan des connaissances actuelles. *Bull. Minéral.*, **106**, 229–46.

Kushiro, I., Yoder, H. S. Jr., and Mysen, B. O. (1976) Viscosities of basalt and andesite melts at high pressures. *J. Geophys. Res.*, **81**, 6351–6.

Lacroix, A. (1893) *Minéralogie de la France*. Libr. Blanchard, réédition 1962, Paris.

Mokhtari, A. and Velde, D. (1988) Xenocrysts in Eocene camptonites from Taourirt. *Mineral. Mag.*, **52**, 587–601.

Potdevin, J.-L. and Marquer, D. (1987) Méthodes de quantification des transferts de matière par les fluides dans les roches métamorphiques déformées. *Geodinamica Acta*, **1**, 3, 193–206.

Rutherford, M. J. (1990) Experimental study of dehydration and crystallization produced by decompression of dacites; implications for magma ascent rates. Program and Abstracts, V.M. Golschmidt Conference, May 2–4, Baltimore, Maryland.

—— and Hill, P. M. (1993) Magma ascent rates from amphibole breakdown: An experimental study applied to the 1980–1986 Mount St. Helens eruptions. *J. Geophys. Res.* (in press).

Shaw, H. R. (1974) Diffusion of H_2O in granitic liquids: Part II. Mass transfer in magma chambers. In *Geochemical transport and kinetics* (Hofmann, A. W., Giletti, B. J., Yoder, H. S. Jr., and Yund, R. A., eds.), Carnegie Inst. Washington, Publ. 634, 155–6.

Tilley, C. E. and Thompson, R. N. (1972) Melting relations of some ultra alkali volanics. *Geol. J.*, **8**, 65–70.

[*Manuscript received 27 July 1992; revised 18 September 1992*]